K. BIDAI*, M. AMERI*,**#, I. AMERI**, D. BENSAID*, A. SLAMANI*, A. ZAOUI***, Y. AL-DOURI****

STRUCTURAL, MECHANICAL AND THERMODYNAMIC PROPERTIES UNDER PRESSURE EFFECT OF RUBIDIUM TELLURIDE: FIRST PRINCIPLE CALCULATIONS

First-principles density functional theory calculations have been performed to investigate the structural, elastic and thermodynamic properties of rubidium telluride in cubic anti-fluorite (anti-CaF$_2$-type) structure. The calculated ground-state properties of Rb$_2$Te compound such as equilibrium lattice parameter and bulk moduli are investigated by generalized gradient approximation (GGA-PBE) that are based on the optimization of total energy. The elastic constants, Young's and shear modulus, Poisson ratio, have also been calculated. Our results are in reasonable agreement with the available theoretical and experimental data. The pressure dependence of elastic constant and thermodynamic quantities under high pressure are also calculated and discussed.

Keywords: Anti-fluorite: Rb$_2$Te; FP-LAPW; GGA; Structural properties; Thermodynamics properties; Elastic constants

1. Introduction

The alkali metal chalcogenides compounds M$_2$A [M: Li, Na, K, Rb; A: O, S, Se, Te] are an important characteristic of these materials that make them technologically useful and interesting as functional materials. These compounds are a good example of homologous series of solids that have predictable physical and physiochemical properties. Rubidium telluride, a unique member of this family, has found potential applications as hybrid photodiode [1-2] for astroparticle physics. Most of the theoretical studies for Rb$_2$Te have been dedicated to their structural properties such as lattice constants and bulk modulus [3-7] or to the phase diagrams of these materials [8-11]. Electronic band structures of Rb$_2$Te compound have been recently predicted by Eithiraj et al. [12] and Seifert-Lorenz and Hafner [13] using Tight-Binding Linear Muffin-tin Orbitals (TB-LMTO) method and pseudopotentials method, respectively, in the frame work of density functional theory DFT. From experimental point of view, absorption spectra [14] at high temperatures and thermodynamic propreties of solutions of Rb$_2$Te in the melt LiCl and LiCl-LiF [15] are also available in literature. At room temperature the Rb$_2$Te compound can crystallize stably into anti-fluorite (anti-CaF$_2$) structure type [16] (space group no. 225). Rb$_2$Te is an exception, which is metastable in anti-CaF$_2$ structure at room temperature and transforms irreversibly to anti-PbCl$_2$ structure type upon warming. The calcium fluoride CaF$_2$ crystal is one of the most common ordered crystals type found in nature and is often termed as fluorite type structure. CaF$_2$ has a basic structure that can be described as face-centered cubic packing of cations, with anions in all of the tetrahedral holes. Contrary to the CaF$_2$ structure, the anti-CaF$_2$ structure has a basic face-centered cubic packing of anions, with cations at the tetrahedral holes. In the Rb$_2$Te compound, the metal atoms (Rb) are located at (1/4; 1/4; 1/4) and (3/4; 3/4; 3/4) positions whereas the Te atom are located at (0; 0; 0) positions. S.M. Alay-e-Abbas and A. Shaukat [17-18] applied the (FP-LAPW) method within generalized gradient approximation (GGA) to study the structure, electronic and optical properties of polymorphic forms of Rb$_2$Te. To the best of our knowledge, there has been no theoretical calculation and experimental data for the elastic constants of Rb$_2$Te reported yet. Moreover, there is a real lack of knowledge of their thermodynamics properties, and elastic properties of Rb$_2$Te under pressure effect up to now. This lack has prompted us to investigate them. This work aims at presenting a first-principles study of the structure, elastic and thermodynamic properties under high pressures of Rb$_2$Te in the anti-fluorite phase. using full potential (linear) augmented plane wave plus local orbital (FP-APW + lo) method within the density functional theory based on Perdew-Burke-Ernzerhof PBE functional. We describe the computational method used in this work in Section 2. The results are discussed in Section 3. Finally, a summary of the work is given in Section 4.

*   LABORATOIRE PHYSICO-CHIMIE DES MATÉRIAUX AVANCÉS (LPCMA), UNIVERSITÉ DJILALI LIABÈS DE SIDI BEL-ABBÈS, SIDI BEL-ABBÈS, 22000, ALGÉRIE.
**   PHYSICS DEPARTMENT, FACULTY OF SCIENCE, UNIVERSITY OF SIDI-BEL-ABBES, 22000-ALGERIA.
***   PHYSIQUE COMPUTATIONNELLE DES MATÉRIAUX, UNIVERSITÉ DJILALI LIABÈS DE SIDI BEL-ABBÈS, SIDI BEL-ABBÈS, 22000, ALGÉRIE.
****   INSTITUTE OF NANO ELECTRONIC ENGINEERING, UNIVERSITY MALAYSIA PERLIS, KANGAR, PERLIS MALAYSIA

Corresponding author. lttnsameri@yahoo.fr

2. Computational methods

The calculations are performed using the FP-LAPW such scalar relativistic approach that is implemented in the WIEN2k [19] code within the framework of density functional theory (DFT) by Hohenberg and Kohn [20] which has been shown to reliable results for the electronic and structural properties of various solids. For the structural properties calculation, for the exchange-correlation potential the generalized gradient approximation (GGA) was used in the form proposed by Perdew et al [21]. In the FP-LAPW method, the wave function of the charge density and potential are developed in spherical harmonic functions inside the muffin-tin spheres and using a plane-wave basis set in space remainder of the unit cell (interstitial region). The muffin-tin radius R_{MT} were assumed to be 2.9 and 3.1 a.u. for Rb and Te atoms respectively. This was done to ensure that the charge will leak the atomic sphere [19]. In this computation, we treated the unit cell with regions divided into interstitial region and non-overlapping muffin tin spheres. We used the plane waves in the interstitial field region and linear combination of radial functions multiplied by spherical harmonics in non-overlapping muffin-tin spheres. We have performed convergence studies and determined the optimum value for cut-off parameter $R_{MT}K_{max} = 9.0$, where R_{MT} is the smallest atomic sphere radius in the unit cell and K_{max} is the maximal value of the reciprocal lattice vector. The k-points for this computation were 750 and the separation energy of the core and valence states was equal to –6.0 Ry.

3. Results and discussion

3.1. Structural properties

In order to calculate the ground state properties of the anti-fluorite Rb$_2$Te compound using GGA (PBE). The ground state bulk properties of the crystals were obtained using the calculations of the total energy as a function of unit cell volume at many different volumes around equilibrium were fitted by the Murnaghan equation of state Murnaghan [22]. The Murnaghan equation is derived, under certain assumptions, from the equations of continuum mechanics. It involves two adjustable parameters, the modulus of incompressibility B and its first derivative with respect to the pressure, B', both measured at ambient pressure. The Murnaghan equationis given by the following expression:

$$E(V) = E_0 + \frac{B}{B'(B'-1)}\left[V\left(\frac{V_0}{V}\right)^{B'} - V_0\right] + \frac{B}{B'}(V - V_0) \quad (1)$$

$$B = V\left(\frac{\partial^2 E(V)}{\partial V^2}\right)_{V_0} \quad (2)$$

and

$$B' = \left(\frac{\partial B}{\partial P}\right)_{P=0} \quad (3)$$

where P is the pressure, V_0 is the equilibrium volume, V is the deformed volume, B is the bulk modulus, and B' is the derivative of the bulk modulus.

The Fig. 1 represents the variation of total energy as a function of volume for Rb$_2$Te. The lattice parameter are in good agreement with the available experimental data of Rb$_2$Te. It is observed that for DFT calculations, the PBE overestimates the values of lattice constant. When we analyse these results of B_0 and B'_0, we find there is a good agreement between our results. These are listed in Table 1. From Table 1 we can see that the calculated value of the bulk modulus B_0 for Rb$_2$Te from the elastic constants ($B_0 = (C_{11} + 2C_{12})/3$) has nearly the value as the one obtained from the equation of state fitting.
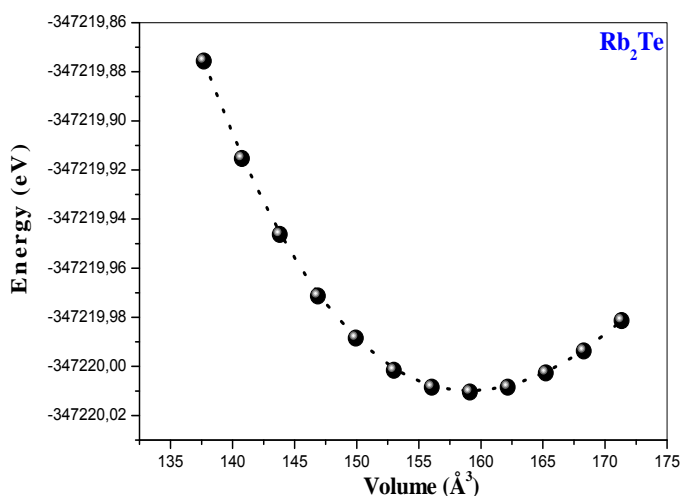

Fig. 1. Total energy as a function of volume for Rb$_2$Te with GGA calculation

TABLE 1

Calculated lattice constant a_0 (Å), bulk modulus B_0 (GPa), its first pressure derivatives B'_0 for Rb$_2$Te, compared to the experimental data and previous theoretical calculations

	Para-meters	Present work	Other calculations	Experi-mental
Rb$_2$Te	a_0	8.603	8.460[b,c] 8.627[b] 8.258[b] 8.4744[d] 8.498[f]	8.490[a]
	B_0	11.465	12.0823[b,c] 12.21[b] 14.69[b] 11.82[d]	—
	B'_0	4.193	4.8394[c] 4.1437[d]	—

[a] Ref. [36], [b] Ref. [35], [c] Ref. [17], [d] Ref. [18], [f] Ref. [7]

3.2. Thermodynamic properties

To evaluate the thermodynamic properties of Rb$_2$Te, we take an approximation method based on quasi-harmonic Debye model [23-24] and combine with the first-principle calculation of E-V relationship to solve the nonequilibrium Gibbs function $G^*(V; P, T)$, which can be expressed as

$$G^*(V, P, T) = E(V) + PV + A_{Vib}(\Theta(V), T) \quad (4)$$

where $E(V)$ is the total energy for per unit cell, PV corresponds to the constant hydrostatic pressure condition, $\Theta(V)$ is the Debye temperature as a function of V, and A_{vib} is the vibrational term which can be written using the Debye model of the phonon density of states as :

$$A_{Vib}\left(\Theta,T\right) = nk_B T\left[\frac{9\Theta}{8T} + 3\ln\left(1 - e^{-\Theta/T}\right) - D\left(\Theta/T\right)\right] \quad (5)$$

where $D(\Theta/T)$ is the Debye integral, and is defined as

$$D\left(\Theta/T\right) = \frac{3}{\left(\Theta/T\right)^3}\int_0^{\Theta/T}\frac{x^3}{e^x - 1}dx \quad (6)$$

where n is the number of atoms per formula unit, Θ the Debye temperature is expressed as [24-26]

$$\Theta = \frac{\hbar}{K}\left[6\pi^2 V^{1/2}n\right]^{1/3} f(\sigma)\sqrt{\frac{B_s}{M}} \quad (7)$$

M being the molecular mass per unit cell, σ Poisson ration and B_S the adiabatic bulk modulus, which is approximated given by the static compressibility:

$$B_s \cong B(V) = V\left(\frac{d^2 E(V)}{dV^2}\right) \quad (8)$$

and the $f(\sigma)$ is given by

$$f(\sigma) = \left\{3\left[2\left(\frac{2(1+\sigma)}{3(1-2\sigma)}\right)^{3/2} + \left(\frac{1+\sigma}{3(1-\sigma)}\right)^{3/2}\right]^{-1}\right\}^{1/3} \quad (9)$$

Therefore, the non-equilibrium Gibbs function $G^*(V; P, T)$ as a function of V, P and T can be minimized with respect to the volume V;

$$\left(\frac{\partial G^*(V,P,T)}{\partial V}\right)_{P,T} = 0 \quad (10)$$

As a result, The isothermal bulk modulus B_T; the heat capacity C_V (at constant volume), and the heat capacity C_P (at constant pressure), and the thermal expansion α are given;

$$B_T(P,T) = V\left(\frac{\partial^2 G^*(V;P,T)}{\partial V^2}\right)_{P,T} \quad (11)$$

$$C_V = 3nk_B\left[4D(\Theta/T) - \frac{3\Theta/T}{e^{\Theta/T} - 1}\right] \quad (12)$$

$$C_P = C_V(1 + \alpha\gamma T) \quad (13)$$

$$\alpha = \frac{\gamma C_V}{B_T V} \quad (14)$$

where the Grüneisen parameter γ is defined as

$$\gamma = -\frac{d\ln\Theta(V)}{d\ln V} \quad (15)$$

In Fig. 2, we present the lattice parameter-temperature diagram at several pressures for Rb_2Te. The lattice parameter increases with increasing temperature at a given pressure. On the other side, as the pressure P increases the lattice parameter decreases at a given temperature. The calculated lattice parameter values for Rb_2Te at room temperature and zero pressure is 8.415 Å.
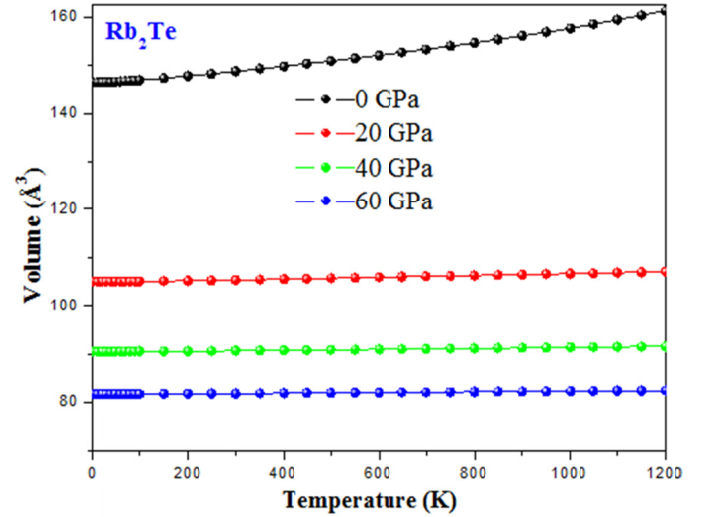

Fig. 2. The variation of the primitive cell volume as a function of temperature at different pressures for Rb_2Te

Fig. 3 shows the bulk modulus variation versus temperature at a given pressure. One can notice that the bulk modulus, a property of a material, which defines its resistance to volume change when compressed, is nearly constant from 0 to 100 K and decreases linearly with increasing temperature for $T > 100$ K. The compressibility increases with increasing temperature at a given pressure and decreases with pressure at a given temperature. At 300 K and zero pressure, the bulk modulus for Rb_2Te is 12.99 GPa.
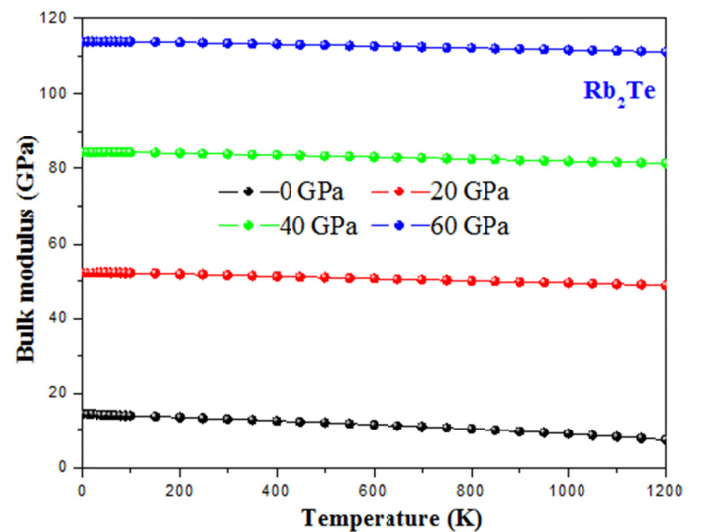

Fig. 3. Temperature dependence of bulk modulus B for Rb_2Te at different pressure

Variation of the heat capacities C_V and C_P versus temperature at 0, 20, 40 and 60 GPa pressures are shown in Figs. 4,5. From 0 to 250 K, C_V and C_P increase exponentially and the difference between them is very slight. At high temperature ($T > 250$ K) C_P follows on a linear increase whereas C_V tends to the Petit and Dulong limit, which is common to all solids at high temperature [27-29]. At high temperature C_V tends to approach 75 Jmol^{-1} K^{-1}. At zero pressure and ambient temperature C_V and C_P are 73.21 and 76.52 Jmol^{-1} K^{-1}, respectively.
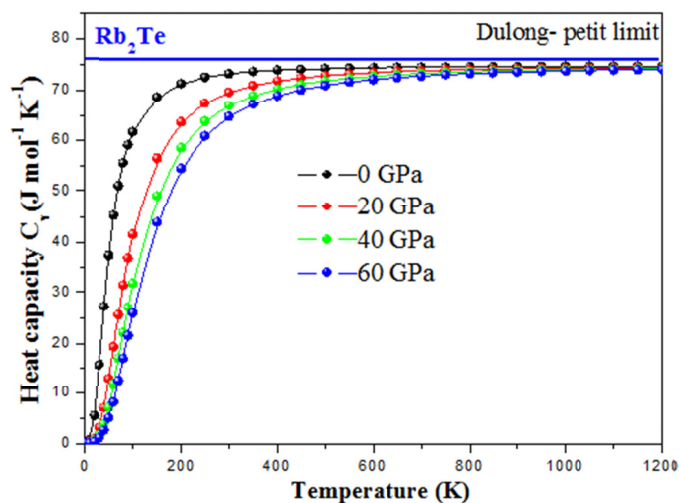

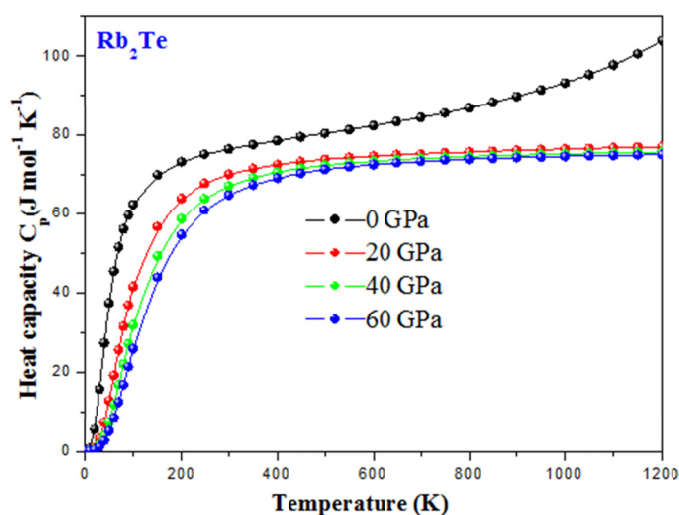Fig. 4. Calculated temperature dependence of heat capacity of Rb$_2$Te at constant volume (C_V)

Fig. 5. Temperature dependence of heat capacity of Rb$_2$Te at constant pressure (C_P)

Further, the variations of the thermal expansion (α), with temperature at various pressures are illustrated in Fig. 6 for Rb$_2$Te. Furthermore, at low temperatures, α enhances rapidly with temperature at zero pressure. The slope of thermal expansion α gradually decreases at higher temperatures at all pressures except at $P = 0$. It should be noted that the thermal expansion coefficient α decreases with the increase of pressure. At $P = 0$ GPa and $T = 300$ K, the values of α for Rb$_2$Te is 6.79×10^{-5} (K^{-1}).
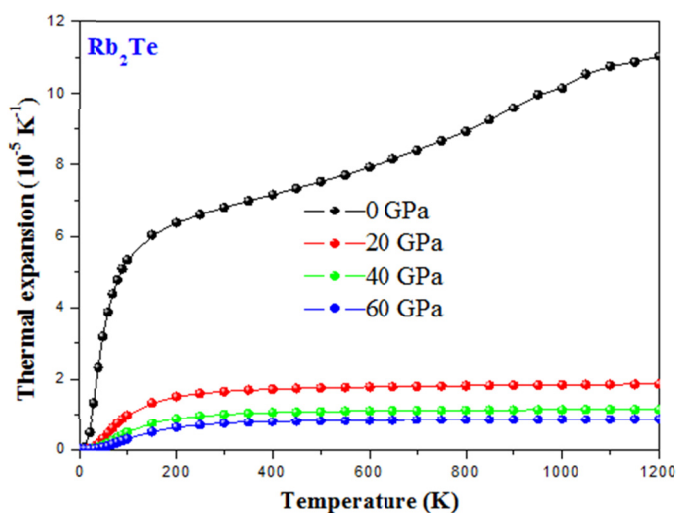

Fig. 6. Thermal expansion as a function of temperature of Rb$_2$Te at different pressure

Fig. 7 displays the dependence of the Debye temperature on temperature and pressure. It can be seen that Debye temperature is nearly constant from 0 to 100 K and decreases linearly with increasing temperature from $T > 100$ K. It is also shown that when the temperature is constant, the Debye temperature increases almost linearly with applied pressure. At zero pressure and 300 K, the obtained Debye temperature values for Rb$_2$Te is 194.87 K.
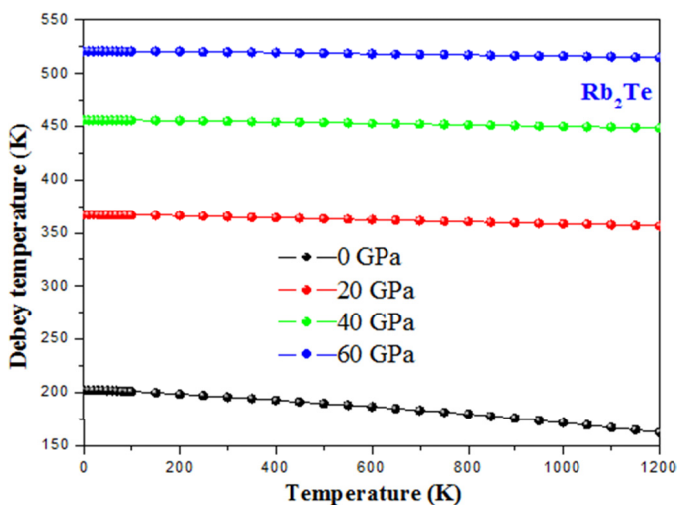

Fig. 7. The variation of the Debye temperature as a function of temperature at different pressures of Rb$_2$Te

The volume dependence of the Debye temperature Θ_D is shown in Fig. 8 at some fixed temperatures. All points lie on a single curve, demonstrating both the consistency of our calculations and the fact that the Debye temperature is a function of the volume only is if bulk modulus varied with Debye temperature the quasi-harmonic approximation which introduces the temperature dependence through the volume and the simplification given by Eq. (7). It is noted that as the volume V increases, the value of the Debye temperature decreases. The relatively small effect of the temperature on the Debye temperature can be explained

by the small effect on the volume changes. It is observed that for constant temperature the Debye temperature of the herein studied materials increases almost linearly with the decrease of the volume.
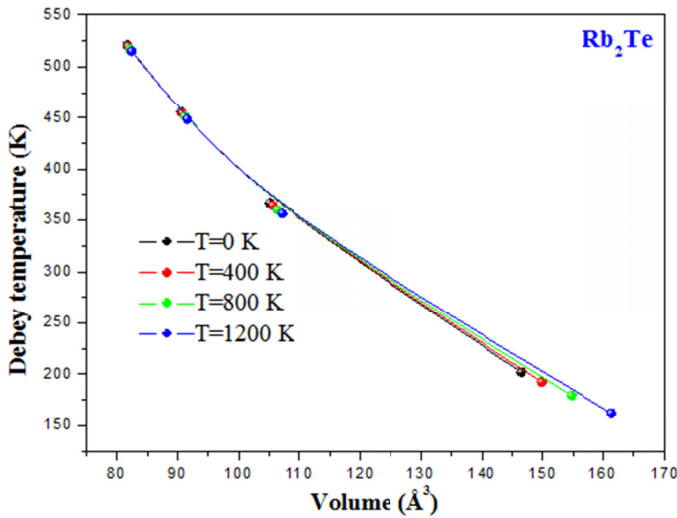

Fig. 8. The variation of the Debye temperature as a function of volume at different pressures of Rb$_2$Te

3.3. Elastic properties

The Rb$_2$Te compound are cubic therefore only three independent elastic constants C_{11}, C_{12} and C_{44} are required to characterize their elastic nature. These constants are important in providing valuable information about the stability and stiffness of materials. The elastic constants C_{ij} are obtained by calculating the total energy as a function of volume conserving strains using Mehl method [30-31] and listed in Table 2. To the best of our knowledge no experimental and theoretical value for the elastic constants of the Rb$_2$Te compound have been published. The traditional mechanical stability conditions of the elastic constants in cubic crystal are known as to be $C_{44} > 0$, $C_{11} > 0$, $C_{11}–C_{12} > 0$, $C_{11} + 2C_{12} > 0$, $C_{12} < B < C_{11}$. The calculated elastic constants for Rb$_2$Te compound are given in Table 2 satisfy these stability conditions in anti-CaF$_2$ structure. Our calculated value of the bulk moduli B_0 from the elastic constants ($B_0 = (C_{11} + 2C_{12})/ = 3$) of Rb$_2$Te is 14.16 GPa; this is nearly the value obtained from fitting the equation of state. The obtained values, within GGA of anisotropic ratio (A), shear modulus (G), Young's modulus (E), Poisson's ratio (v) and B/G ratio are given in Table 3 for Rb$_2$Te. Since here are no available experimental result for this compound.

TABLE 2

Calculated elastic constants (in GPa) for Rb$_2$Te in anti-CaF2 structure

	Parameters	Present work
Rb$_2$Te	C_{11}	22.12
	C_{12}	10.19
	C_{44}	7.923

TABLE 3

Calculated Zener anisotropy factor A, Poisson's ratio v, shear modulus G (in GPa), Young's modulus E (in GPa)

Material		G	E	A	B/G	v
Rb$_2$Te	Present work: GGA	7.07	18.19	1.32	2.00	0.28

The elastic anisotropy of crystals has an important implication in engineering science since it is highly correlated with the possibility to induce micro cracks in the materials. To quantify the elastic anisotropy for this compound, we have calculated the anisotropy factor A is given as:

$$A = \frac{2C_{44}}{C_{11} - C_{12}} \tag{16}$$

from the present calculated values of the elastic constants. For a completely isotropic material, A is equal to the unity, while any value smaller or larger than unity indicates anisotropic characteristic. The magnitude of the deviation from unity measures the degree of elastic anisotropy possessed by the crystal. The calculated value of the anisotropic factor A listed in Table 3. As can be seen from the Table 3, the Rb$_2$Te cannot be regarded as elastically isotropic due to the A values larger than 1.0.

Young's modulus (E) and Poisson's ratio (v), which are the most interesting elastic properties for application, are also calculated in terms of the computed data using the following relations [32]

$$E = \frac{9BG}{3B + G} \tag{17}$$

and

$$v = \frac{3B - 2G}{6B + 2G} \tag{18}$$

Poisson's ratio provides more information about the characteristic of the bonding forces than any of the other elastic constants. 0.25 [33] and 0.5 are the lower and upper limits for central force solids. The calculated Poisson ratio of Rb$_2$Te is very close to 0.28, which means that Rb$_2$Te is with predominantly central inter-atomic forces
Where $G = (Gv + G_R)/2$ is the anisotropic shear modulus, Gv is the Voigt shear modulus corresponding to the upper bound of G values, and G_R is the Reuses shear modulus corresponding to the lower bound of G values. For a cubic crystal Gv and G_R are given as:

$$G_V = \frac{(C_{11} - C_{12} + 3C_{44})}{5} \tag{19}$$

and

$$G_R = \frac{5(C_{11} - C_{12})C_{44}}{4C_{44} + 3(C_{11} - C_{12})} \tag{20}$$

Following the Pugh criterion [34], the critical value of the ratio B/G separating the ductile and brittle behaviour of materials is around 1.75; i.e. if B/G. 1.75, the material behaves in a ductile

manner; otherwise the material behaves in a brittle manner, the Rb_2Te compound is classified as a ductile material.

We further study the high-pressure elastic behavior of the Rb_2Te by computing the second-order elastic constants and their variation with pressure, as shown in Fig. 9. We can see that C_{11}, C_{12}, and C_{44} increase linearly with pressure P. C_{11} and C_{12} are more sensitive to the change of pressure compared to C_{44}.
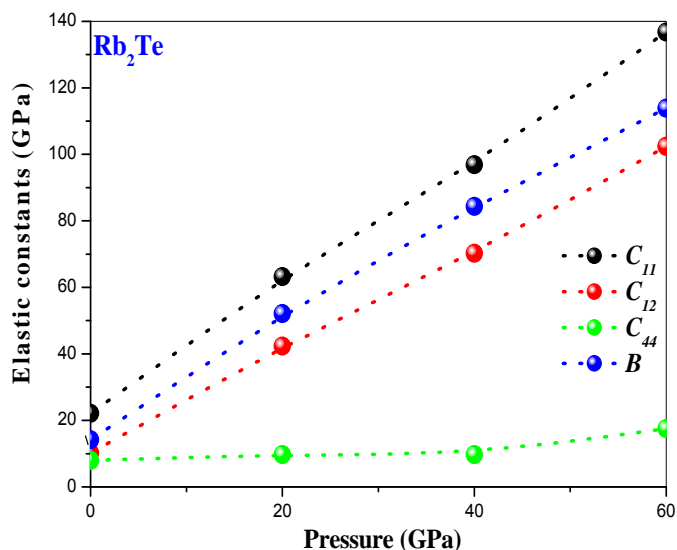

Fig. 9. Pressure dependence of the elastic constants (C_{11}, C_{12} and C_{44}) and B of Rb_2Te

4. Conclusion

In this work, we have calculated the ground-state structural, elastic and thermodynamic properties of Rb_2Te in the anti-fluorite structure by means of using full-potential augmented plane wave plus local orbitals method (FP-LAPW+ lo) within density functional theory, using generalized gradient approximation (GGA). The results of ground state structural properties are in good agreement with available theoretical and experimental studies. We have also calculated and presented the elastic constants C_{ij} under high pressure. Using the quasi harmonic Debye model, some basic thermodynamical quantities such as the lattice parameter, bulk modulus, the specific heat capacity, thermal expansion coefficient and Debye temperature as a function of temperature are calculated at the pressure of 0-60 GPa and temperature of 0-1200 K, and the results are also interpreted. To our knowledge, this is the first quantitative theoretical prediction for the elastic and thermodynamic properties for the investigated compound.

REFERENCES

[1] A. Braem, E. Chesi, C. Joram, J. Séguinot, P. Weilhammer, M. Giunta, N. Malakhov, A. Menzione, R. Pegna, A. Piccioli, F. Raffaelli, G. Sartori, Development of a 10-inch HPD with Integrated Readout Electronics, Nucl. Instr. Meth. Phys. Res. Sect. A **504**, 19 (2003).

[2] A. Piccioli, R. Pegna, I. Fedorko, M. Giunta, N. Malakhov, A. Menzione, F. Raffaelli, A. Braem, E. Chesi, C. Joram, J. Séguinol, G. Sartorl, P. Weilhammer, Characterization of a potted 5-in. HPD with Rb2Te photocathode, Nucl. Instr. Meth. Phys. Res. Sect. A **518**, 602-604 (2004).

[3] A.K. Koh, Phys. systematic Variation between Cohesive Energy and a lattice ratio in alkali chalcogenide crystalsm, Status Solidi B **210**, 31 (1999).

[4] V.K. Jain and J. Shanker; Relative stability and structural phase-transitions in alkaline-earth chalcogenide crystals, Phys. Status Solidi B **114**, 287 (1982).

[5] S.D Chaturvedi, S.B, Sharma, P. Paliwal, M. Kumar, Phys. analysis of crystal binding and structural phase transition in alkaline-earth and alkali chalcogenides, Status Solidi B **156**, 171 (1989).

[6] A. Melillou, B.R.K. Gupta Czechoslovak. cohesive and elastic properties of alkaline earth chalcogenide crystals, Journal of Physics **41**, 813 (1991).

[7] K. Stowe, Z. Kristallogr. **219**, 359 (2004).

[8] J. Sangster, A.D. Pelton, The li-Te (lithium-tellurium) system, J. Phase. Equilib. **3**, 300-303 (1992).

[9] A.D Pelton, A. Petric, The Na-Te (Sodium-Tellurium) system (Citations: 3). J. Phase. Equilib. **11**, 447-451 (1990).

[10] A. Petric, A.D. Pelton, The K-Te (Potassium-Tellurium) system (Citations: 2), J. Phase. Equilib. **11**, 443-447 (1990).

[11] J. Sangster, A.D. Pelton, The Rb-Te (rubidium-tellurium) system, J. Phase. Equilib. **18**, 394-396 (1997).

[12] R.D. Eithiraj, G. Jaiganesh, G. Kalpana, First-principales study of electronic structure and ground-state properties of alkali-metal selenides and tellurides (M_2A)[M: Li, Na, K; A: Se, Te], Int. J. Mod. Phys. B **23**, 5027 (2009).

[13] K. Seifert-Lorenz, J. Hafner, Crystalline intermetallic compounds in the K-Te system: The Zintl-Klemm principle revisited, Phys. Rev. B **66**, 094105 (2002).

[14] D.M. Gruen, R.L. McBeth, M.S. Foster, C.E. Crouthamel, Absorption Spectra of Alkali Metal Tellurides and of Elemental Tellurium in Molten Alkali Halides, J. Phys. Chem. **70**, 472-477. (1966).

[15] M.S. Foster, C.C. Liu, Free Energy of Formation of Li_2Te at 798°K by an Electromotive Force Method, J. Phys. Chem. **7**, 950-952 (1966).

[16] E. Zintle, A. Harder, B. Dauth, Lattice Structure of the oxides, sulfides, selenides and tellurides of lithium, sodium and potassium, Z. Elektrochem. **40**, 588 (1934).

[17] S.M. Alay-e-Abbas and A.Shaukat, FP-LAPW calculations of structural, electronic and optical properties of Alkali metal tellurides: M_2Te [M : Li, Na, K and Rb], J. Mater. Sci. **46**,1027-1037 (2011).

[18] S.M. Alay-e-Abbas and A. Shaukat, First principles study of structural, electronic and optical properties of polymorphic forms of Rb$_2$Te. Solid State Sciences **13**, 1052-1059 (2011).

[19] P. Blaha, K. Schwarz, G.K.H. Madsen, D. Kvasnicka, J. Luitz, Wien2k. An Augmented Plane Wave plus local Orbitals Program for Calculating Crystal Properties, Karlheinz Schwarz, Techn. Universitat Wien, Austria, 2001, (ISBN 3-9501031-1-2).

[20] P. Hohenberg, W. Kohn, Inhomogeneous electron gases, Phys. Rev. B **864**, 136 (1964).

[21] P. Perdew, S. Burke, M. Ernzerhof, Generalized Gradient Approximation Made Simple, Phys. Rev. Lett. **77**, 3865 (1996).

[22] F.D. Murnaghan, The Compressibility of Media under Extreme Pressures, Proc. Natl. Acad. Sci. USA **30**, 244 (1944).

[23] Y. Zhang, X. Ke, C. Chen, J. Yang, P.R.C. Kent, Thermodynamic properties of PbTe, PbSe, and PbS: First-principles study, Phys. Rev. B **80**, (2009) 024304.

[24] M.A. Blanco, E. Francisco, V. Luaña, GIBBS: Isothermal-Isobaric Thermodynamics of Solids from Energy Curves Using a Quasi-Harmonic Debye Model, Comput. Phys. Com. **158**, 57-72 (2004).

[25] M.A. Blanco, A. Martin Pendas, E. Francisco, J.M. Recio, R. Franco, Thermodynamical properties of solids from microscopic theory: applications to MgF$_2$ and Al$_2$O$_3$, J. Molec. Struct. Theochem. **368**, 245 (1996).

[26] M. Florez, J.M. Recio, E. Francisco, M.A. Blanco, A. Martin Pendas, First-principles study of the rock salt-cesium chloride relative phase stability in alkali halides, Phys. Rev. B **66**, (2002) 144112.

[27] T. Belaroussi et al, First-principles study of the structural and thermodynamic properties of AsNMg3 antiperovskite, Physica B **403**, 2649-2653 (2008).

[28] L.Y. Lu, Y. Cheng, X.R. Chen, J. Zhu, Physica B **370**, 236 (2005).

[29] J. Chang, X.R. Chen, W. Zhang, J. Zhu, Chin. First-principles investigations on elastic and thermodynamic properties of zinc-blende structure BeS, Phys. B **17**, 1377 (2008).

[30] M.J. Mehl, J.E. Osburn, D.A. Papaconstantopoulos, B.M. Klein, Structural properties of ordered high-melting-temperature intermetallic alloys from first-principles total-energy calculations, Phys. Rev. B **41**, 10311 (1990).

[31] M.J. Mehl, B.M. Klein, D.A. Papaconstantopoulos, Intermetalic Compounds: Principles and Practice in: J.H. West-Brook, R.L. Fleisher (Eds.), Principles Intermetallic Compounds, Wiley, New York **1**, 195-210 (1995).

[32] R. Hill, The Elastic Behaviour of a Crystalline Aggregate, Pro. Phys. Soc. London **65**, 350 (1953).

[33] J. Haines, J.M. Leger, G. Bocquillon, Synthesis and design of superhard materials, Annu. Rev. Mater. Res. **31**,1-23 (2001).

[34] S.F. Pugh, Predicted studies of semiconductors, Philos. Mag. **45**, 823-843 (1954).

[35] S.M. Alay-e-Abbas, N. Sabir, Y. Saeed, A. Shaukat, First-principles study of structural and electronicproperties of alkali metal chalcogenides: M$_2$Ch [M: Li, Na, K, Rb; Ch: O, S, Se, Te], Int. J. Mod. Phys. B **25**, 3911-3925 (2011).

[36] K. May, Z. Kristallogr. **94**, 412 (1936).